

## Emission of $K$ X Rays and Division of Nuclear Charge in the Spontaneous Fission of $^{252}\text{Cf}$ †

S. S. KAPOOR,\* H. R. BOWMAN, AND S. G. THOMPSON

*Lawrence Radiation Laboratory, University of California, Berkeley, California*

(Received 21 July 1965)

Measurements of the energies of the prompt  $K$  x rays emitted by the fragments in the spontaneous fission of  $^{252}\text{Cf}$  have been made which give information concerning the division of nuclear charge in fission. The kinetic energies of the pairs of fragments and the coincident  $K$  x rays emitted along the direction of fragment motion were recorded event by event, using a multiparameter analyzer. The energies of the fragments were measured by two semiconductor detectors, and the x-ray energies were measured with a lithium-drifted silicon detector operated at dry-ice temperature. The energy resolution of the x-ray detector as measured in terms of the full width at half-maximum of the 59.57-keV line of  $^{241}\text{Am}$  was 3.5 keV. The data were analyzed to obtain (a) the most probable charge versus the fragment mass, (b) the x ray yield per fragment versus the fragment mass and charge, and (c) the average half-life for x-ray emission versus the fragment mass and charge. The measured x-ray emission times and the variation of the x-ray yield per fragment with the fragment mass are found to be consistent with the view that these x rays are emitted as a result of the internal-conversion process during the de-excitation of the fragment nuclei. In the heavy group, the abrupt rise in the x-ray yield at fragment mass 144 appears to be connected with the onset of large stable nuclear deformations of fragment nuclei at neutron number about 88. The measured x-ray yield from the light-fragment group suggests that most of these nuclei make up a new region of deformation. The observed variation of the most probable charge with the fragment-mass ratio over a limited mass region is found to be very similar to that obtained in radiochemical studies of the thermal fission of  $^{235}\text{U}$ .

### I. INTRODUCTION

THE study of the nuclear charge division in the fission process has been, until recently, mainly carried out using radiochemical methods<sup>1</sup> to identify the mass and charge of the fission products. From earlier work,<sup>2-4</sup> however, it was known that the fragments emit characteristic  $K$  x rays; therefore, coincident measurements of the energies of these x rays and the masses of the emitting fragments could in principle provide a direct physical determination of the nuclear charges.

The availability of high-resolution solid-state detectors and multiparameter systems have made it convenient to carry out these studies. A measurement of the nuclear charges of the fragments from a study of the characteristic  $K$  x rays is also reported in the preceding article by Glendenin and Unik,<sup>5</sup> in which the energies of the  $K$  x rays were measured perpendicular to the direction of motion of the fragments using a thin NaI(Tl) scintillator and by an argon-filled proportional counter.

† This work was done under the auspices of the U. S. Atomic Energy Commission.

\* On leave from the Atomic Energy Establishment, Trombay, India.

<sup>1</sup> A. C. Wahl, R. L. Ferguson, D. R. Nethaway, D. E. Troutner, and K. Wolfsberg, *Phys. Rev.* **126**, 1112 (1962).

<sup>2</sup> V. V. Skliarevskii, D. E. Fomenko, and E. D. Stepanov, *Zh. Eksperim. i Teor. Fiz.* **32**, 256 (1957) [English transl: *Soviet Phys.—JETP* **5**, 220 (1957)].

<sup>3</sup> V. K. Voetovetskii, B. A. Levin, and E. V. Marchenko, *Zh. Eksperim. i Teor. Fiz.* **32**, 263 (1957) [English transl.: *Soviet Phys.—JETP* **5**, 184 (1957)].

<sup>4</sup> R. B. Leachman, *Proceedings of the Second United Nations International Conference on the Peaceful Uses of Atomic Energy, Geneva, 1958* (United Nations, Geneva, 1958), Vol. 15, p. 331.

<sup>5</sup> L. E. Glendenin and H. C. Griffin, *Phys. Letters*, **15**, 153 (1965); L. E. Glendenin and J. P. Unik, preceding article, *Phys. Rev.* **140**, 1301 (1965).

In the present work, the x-ray energies were measured using a high-resolution lithium-drifted silicon detector. The x rays were detected in the direction of motion of the fragments. Since the geometry varies as a function of position, estimates of the half-life for x-ray emission could be made from the ratio of the intensities of the x rays observed at  $0^\circ$  and at  $180^\circ$  with respect to the direction of motion of the emitting fragment. The kinetic energies of the fragments and the energies of the coincident  $K$  x rays were recorded event by event in correlated form and the data were analyzed to obtain (a) the values of the most probable charge versus the fragment mass, (b) the x-ray yield per fragment versus the fragment mass and charge and (c) an estimate of the average half life for x-ray emission versus the fragment mass and charge. The results concerning the time of emission and the yield of the x rays are found to be consistent with the view that these  $K$  x rays are emitted as a result of the internal-conversion process which takes place during the gamma de-excitation of the fragments. The observed variation of the charge density with the fragment mass ratio is found to be similar in certain respects to that obtained by radiochemical studies<sup>1</sup> of the thermal neutron induced fission of  $^{235}\text{U}$ .

### II. EXPERIMENTAL

#### A. Apparatus

A schematic diagram of the experimental arrangement is shown in Fig. 1. A weightless amount of  $^{252}\text{Cf}$  deposited onto a thin nickel foil by the self-transfer technique was used in the measurements. The kinetic energies of the pairs of fragments were measured by two diffused-junction silicon detectors of 0.05-cm thick-

ness, placed at a distance of about 1.9 cm on either side of the source foil. A lithium-drifted silicon detector with a depletion depth of 0.3 cm was mounted in line with the fragment detectors, at a distance of 3.8 cm from the source foil, to measure the energies of the  $K$  x rays emitted along the direction of motion of the fragments. This geometry was chosen to provide a significant difference in the solid angles of detection of the x rays emitted by fragments moving toward the counter as compared to those for detection of x rays from fragments moving away from the counter. The x-ray detector was operated near dry ice temperature, and with a reverse bias of 600 V to obtain the best energy resolution. This energy resolution measured in terms of the full width at half-maximum (FWHM) of the 59.57-keV line of  $^{241}\text{Am}$  was 3.5 keV.

## B. Electronics

### 1. General

A simplified block diagram of the electronic arrangement is shown in Fig. 1. The pulses from each detector preamplifier were fed to a standard transistorized amplifier and then to a triple coincidence unit of the zero cross-over type. For the pulses from the x-ray detector, the single-channel analyzer preceding the coincidence unit was set with its base line at about 10 keV to cut off the detector noise and with its upper level at about 80 keV to avoid recording the fission gamma rays of higher energies. The time resolution of the coincidence unit was set at 50 nsec, and therefore, the present measurements are restricted to the prompt x rays emitted within 50 nsec after fission. The amplifier outputs of the detectors were gated by the triple-coincidence pulse, and the gated-output pulses were stored in the correlated form in temporary memory No. 1. The three pulse heights were then analyzed serially by the pulse-height analyzer, and the outputs of the analyzer were in turn stored in memory No. 2, event by event, so that the order of the detector pulses was maintained. The output of memory No. 2 was written on a magnetic tape, each time memory No. 2 became full. The magnetic tape could be read back at the end of each run to observe the data just as it came and also to determine the spectrum of the pulses from each of the detectors.

### 2. Gain Stabilization

To avoid any possible contributions of electronic drift to the output pulse heights during the long runs of the experiments, digital-stabilizer units of the type described by Nakamura *et al.*<sup>6</sup> were incorporated in the electronic system. The output pulse heights from the x-ray detector system were stabilized with the 59.57-keV gamma-ray line of  $^{241}\text{Am}$ , the source being

<sup>6</sup> M. Nakamura and R. LaPierre, Lawrence Radiation Laboratory Report UCRL-11494, 1964 (unpublished).

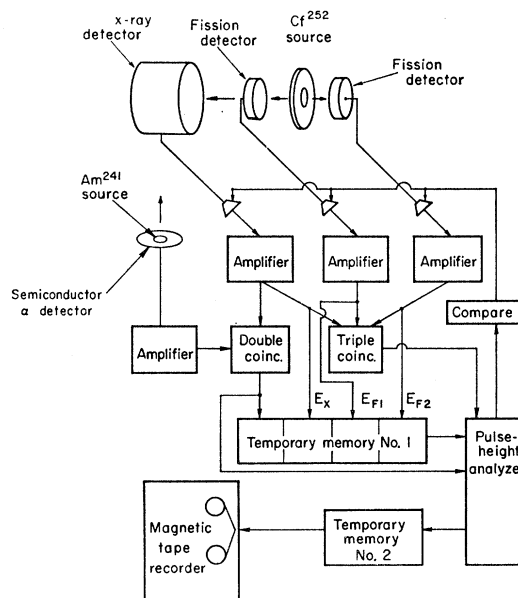


Fig. 1. Schematic diagram of the experimental arrangement and the block diagram of the electronic system.

mounted between the x-ray detector and a semiconductor alpha detector (Fig. 1). Whenever a double coincidence between the pulse from the alpha detector and the pulse from the x-ray detector corresponding to the 59.57-keV gamma-ray line occurred, a fixed pulse height was fed to the fourth dimension of the analyzer to label the stabilizing events. The number of these gated pulses corresponding to the  $^{241}\text{Am}$  gamma-ray line occurring in a preselected peak were monitored in a reversible scaler, which gave the difference in the number of pulses appearing above and below the preselected peak channel. The analog voltage corresponding to the scaler's content was fed back to the variable-gain amplifier preceding the main amplifier to correct for the gain changes and thereby to stabilize the gain of the system. The gain of each of the systems corresponding to the fission fragment detectors was stabilized in a similar way. The stabilizing pulse was obtained from a scaler after every  $10^8$  double coincidence events, and a different fixed pulse height was fed to the fourth dimension to label these events. This also enabled a simultaneous recording of the double-coincidence data corresponding to the pulse heights of the two fragments (without regard to the x rays). With the incorporation of the stabilizing system, no drift in the system gain was detected even after months of operation. The pulse-height dispersion introduced by the stabilizing system was always less than about 0.1%.

## C. X-Ray Detection Efficiency and Energy Calibration

The x-ray intensities were attenuated in passing through the fission fragment detectors in the present

experimental arrangement. The transmission  $T(E)$  of the x rays of different energies was calculated using the known values of the fragment detector thickness and the absorption coefficients for silicon. The transmission of x rays of different energies was also measured experimentally and was found to be in agreement with the calculated values. The photopeak efficiencies  $\eta(E)$  of the x-ray silicon detector were calculated for x rays of different energies from the known photoelectric and total absorption cross sections. From this the total detection efficiency defined by  $\eta_T(E) = \eta(E)T(E)$  was obtained. The absolute value of the efficiency  $\eta_T(E)$  was also measured with photons of energy 59.57 keV from  $^{241}\text{Am}$ , using the value 0.359 given by Magnusson<sup>7</sup> for the number of photons emitted per alpha. The measured value of  $\eta_T(E)$  was found to agree with the calculated value. The calculated values of  $\eta_T(E)$  versus photon energy  $E$  were used to obtain the absolute x-ray yield from the measured yield. The relation between the output pulse heights from the x-ray detector system and the x-ray energies was determined using a high-precision pulser which was in turn calibrated with respect to energy using the 59.57-keV photons from  $^{241}\text{Am}$ .

The chance coincidence rate between the double-coincidence pulses from the two detectors and the pulses from the x-ray detector was obtained by inserting appropriate delays in the x-ray detector channel and was found to be about one percent. However, the major source of background was found to be due to the true coincidences occurring between the fragments and the Compton-scattered fission gamma rays. The silicon detector for x-ray detection was selected to minimize this Compton background.

#### D. Data Collection and Sorting

In the present experiments, about  $1.2 \times 10^6$  events were recorded on the magnetic tape. About 85% of the events were the triple coincidences between the two fragment pulses and the associated pulse from the x-ray detector; 10% were the double-coincidence events between the two fragments, and the rest were the stabilizing pulses from  $^{241}\text{Am}$ .

The coincident pulse-height data gathered in the experiments were processed on the IBM-7094 computer. The labeling in the fourth dimension of the double coincidence and the stabilizing pulses enabled the separation of these events from the main triple-coincidence data. The fragment detector systems were calibrated into energies by normalizing the first moments of the pulse-height distributions (double-coincidence data) to the first moments of the respective distributions obtained by the time-of-flight measurements of Fraser *et al.*<sup>8</sup> The fission fragment masses were calculated using

the relation  $M_1E_1 = M_2E_2$ , where  $M$  and  $E$  are the fragment mass and kinetic energy before the emission of neutrons. Since the measured fragment kinetic energies correspond to the fragment masses after the emission of neutrons, these values were corrected to obtain initial kinetic energy of the fragments using the data on the average number of neutrons emitted as a function of the fragment mass and total kinetic energy of the fragments as measured by Bowman *et al.*<sup>9</sup> An iterative type of calculation was done to obtain the fragment masses and total kinetic energies before and after neutron emission. The main triple-coincidence data were then sorted on the computer to obtain the energy distributions of the x rays for the cases when the fragments of mass  $M_f$  (after the emission of neutrons) were moving at  $0^\circ$  and at  $180^\circ$  to the direction of detection of the x rays. The x-ray distributions were obtained for the fragment masses lying within the interval of two mass units.

### III. EXPERIMENTAL RESULTS

The energy spectra of the K x rays observed from all the fragments is shown in Fig. 2. Figure 3 shows a three-dimensional model of the observed energy distributions of the x rays for 32 intervals of the fragment masses moving toward the x-ray detector. The typical observed spectra of the x rays when the fragments in the mass ( $M_f$ ) range 139–141 are moving toward and away from the x-ray detector are shown by the solid and dotted line respectively in Fig. 4. The fact that the average energy of the x rays in the two cases are different shows that most of the x rays are emitted from the moving fragments, and consequently, undergo Doppler shift in the energy. Secondly, the fact that the intensity of the x rays detected is significantly greater when the emitting fragment is moving towards the detector shows that these x rays are emitted all along

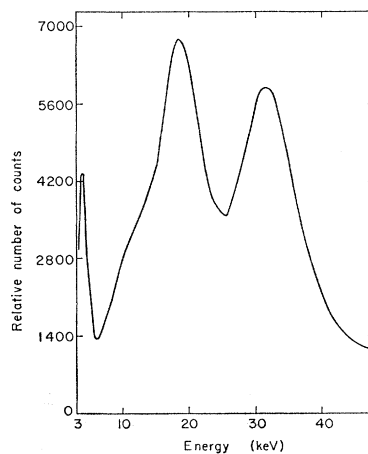


FIG. 2. Energy spectrum of the K x rays observed in coincidence with all the fragments. This spectrum contains x rays emitted from both members of the fragments, one moving toward the detector and the other moving away from it.

<sup>7</sup> L. B. Magnusson, Phys. Rev. **107**, 161 (1957).

<sup>8</sup> J. S. Fraser, J. C. D. Milton, H. R. Bowman, and S. G. Thompson, Can. J. Phys. **41**, 2080 (1963).

<sup>9</sup> H. R. Bowman, S. G. Thompson, J. C. D. Milton, and W. J. Swiatecki, Phys. Rev. **126**, 2120 (1962).

the fragment path with the average position of the x-ray emission away from the foil.

It can be seen from Figs. 3 and 4 that the observed x-ray peaks are superimposed on a small background due to the Compton-scattered fission gamma rays. The main contribution to the width of these x-ray peaks comes from the following factors: (a) the experimental x-ray energy resolution, (b) the experimental mass resolution, (c) the charge distribution for a single fragment mass, and (d) the fact that for each value of  $Z$ , different x-ray energies arise due to the  $K\alpha_1$ ,  $K\alpha_2$ ,  $K\beta_1$ , and  $K\beta_2$  transitions.

#### A. Determination of $Z_p$ versus $A_i$

From the observed x-ray energy distributions associated with the fragments of average final mass  $M_f$  moving toward and away from the x-ray detector, the

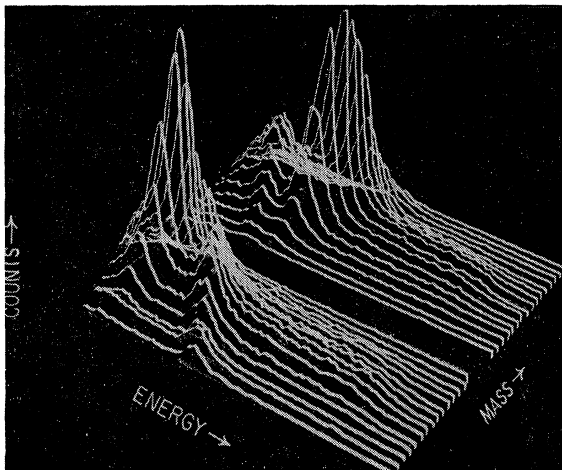


FIG. 3. A three-dimensional model of the observed energy spectra of the prompt  $K$  x rays for 36 intervals of the fragment masses moving toward the x ray detector.

x-ray peak energies  $E_1$  and  $E_2$ , respectively, for the two cases were obtained. An estimate of the accuracy of these measurements was obtained by also analyzing the spectra associated with the average mass  $M_f^c$ , complementary to  $M_f$ , for obtaining the peak energies  $E_1'$  and  $E_2'$ , when the fragments of mass  $M_f^c$  were moving away and toward the x-ray detector, respectively. As both  $E_1$ ,  $E_1'$  and  $E_2$ ,  $E_2'$  are the measurement of the same quantities by two different plots, the measured differences  $|E_1 - E_1'|$  and  $|E_2 - E_2'|$  give an estimate of the uncertainty in determining the peak energies. Also from this the average values  $\bar{E}_1$  and  $\bar{E}_2$  of the two measurements were obtained. The estimated uncertainty in the values of  $\bar{E}_1$  and  $\bar{E}_2$  was about 0.1 keV. The peak energy  $E_x$  of the x rays in the fragment system was obtained by the relation

$$E_x = (\bar{E}_1 + \bar{E}_2)/2.$$

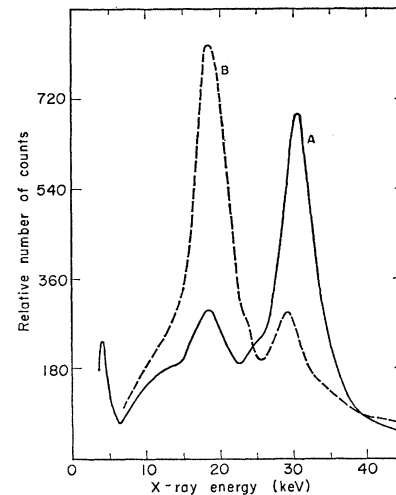


FIG. 4. The measured energy distributions of the  $K$  x rays for the cases of the fragments in the mass interval 139–141 moving (a) toward and (b) away from the x-ray detector.

For each value of  $Z$ , the expected x-ray energy distribution curve was computed by adding four Gaussian distributions, corresponding to the  $K\alpha_1$ ,  $K\alpha_2$ ,  $K\beta_1$ , and  $K\beta_2$  transitions, each having the FWHM corresponding to the observed energy resolution and having average energies and relative intensities as given by Wapstra *et al.*<sup>10</sup> The plot of the peak energies of the computed curve versus  $Z$  was used to obtain the most probable charges  $Z_p$  associated with the measured values of  $E_x$ . The average masses  $M_f$  were corrected for the effect of mass dispersion using the method of Terrell,<sup>11</sup> with 2.25 for the variance  $\sigma_{M_f}$  as directly measured in the earlier experiments<sup>12</sup> on the gamma-ray emission. The average initial fragment mass  $A_i$  was obtained from the corrected mass  $M_f^*$  using the known average values for the number  $\bar{\nu}$  of neutrons emitted. The values of the most probable charge  $Z_p$  versus the initial mass  $A_i$  of the fragments, obtained in this way, are shown in Fig. 5,<sup>13,14</sup> where the measured charges and masses of the light and heavy fragments are plotted on a complementary scale. The fact that the data points corresponding to the light and the heavy fragments describe the same curve, shows that the sum of the measured charges of the complementary fragments do add up to 98 within the experimental uncertainty of about 0.2 units. The sum of the charges of the complementary fragments, averaged over all the events, was actually found to be  $(97.9 \pm 0.2)$ .

A few general comments can be made here concerning

<sup>10</sup> A. H. Wapstra, G. J. Nijgh, and R. Van Lieshout, *Nuclear Spectroscopy Tables* (North-Holland Publishing Company, Amsterdam, 1959).

<sup>11</sup> J. Terrell, *Phys. Rev.* **127**, 880 (1962).

<sup>12</sup> H. R. Bowman, S. G. Thompson, R. L. Watson, S. S. Kapoor, and J. O. Rasmussen, *Proceedings of the International Symposium on the Physics and Chemistry of Fission*, Salzburg, Austria, 1965 (unpublished).

<sup>13</sup> Hiroshi Baba (private communication).

<sup>14</sup> C. D. Coryell, R. A. Brightsen, and A. C. Pappas, *Phys. Rev.* **85**, 732 (1952); C. D. Coryell, *Ann. Rev. Nucl. Sci.* **2**, 305 (1953).

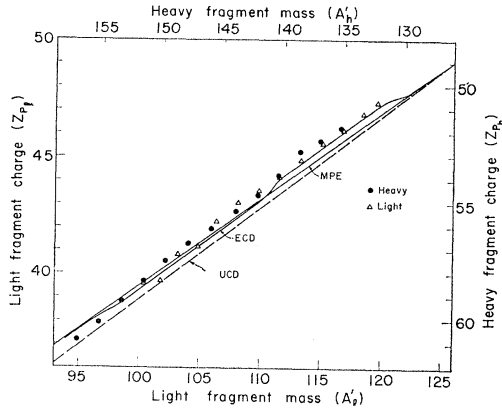


FIG. 5. The most probable charge ( $Z_p$ ) versus the initial mass of the fragments ( $A_i$ ) (corrected for mass dispersion) as determined from the x ray measurements. The curves calculated under the hypothesis of unchanged charge density (UCD), equal charge displacement (ECD) as applied to the fragments before the emission of neutrons and the minimum potential energy postulate (MPE) are also shown in the figure. UCD hypothesis implies that the ratio of neutron to proton in each of the fragments is equal to that of the fissioning nucleus. In calculating the ECD curve the values of the stable charges were taken from the treatment of  $\beta$  stability by Coryell *et al.* (Ref. 14) and at the shell crossings the average of the charge values from the two shell groups were used. The curve MPE is taken from the work of Hiroshi Baba (Ref. 13), in which the most probable charges are calculated by minimizing the potential energy of two touching ellipsoids with respect to both the charge division and the eccentricities of the ellipsoids, and thus, for each mass division, the charges corresponding to the lowest potential energy configuration are obtained. The nuclear shape-dependent mass formula of Myers and Swiatecki (Ref. 22) was used in the calculations.

the present measurement of the most probable charges from the x-ray energy measurements. As discussed later, it is reasonable to assume that internal conversion during the gamma de-excitation of the fragments is the main process giving rise to the emission of  $K$  x rays. Now, if the transitions involved are such that there exist large discontinuous changes in the x-ray yield in going from one nuclide to another, the different charges corresponding to  $P(Z)$  distribution for each  $A_i$  and the different  $A_i$  corresponding to the distribution  $P(A_i)$  in the selected mass interval of 2 units, may not be weighted equally leading to the average most probable charge  $Z_p$  and mass  $A_i$  somewhat different from the true ones. However, in such a case it would be very unlikely that the sum of the measured charges of the complementary fragments should add up to 98. On the basis of this evidence alone it appears that no noticeable biasing in the measured  $Z_p$  values exists; this is reasonable on the basis that large discontinuous changes in the x-ray yield are generally not expected for slightly differing  $Z$  and  $A_i$  values in the  $P(Z)$  and  $P(A_i)$  distributions, possibly due to the conversion of several transitions in each nuclide. We do observe, for one case, where for average mass  $A_i \approx 102$ , there is a slight discontinuity in the values of the light and heavy fragment charges. Though this could be assigned to the possible biasing of  $Z_p$  values in this mass interval,

certain other possibilities like the presence of a discontinuity in this region in the  $\bar{\nu}$  versus  $A_i$  curve or  $Z_p$  versus  $A_i$  curve itself cannot be ruled out. In general, the present results point to the suitability of this method for determining the most probable charges of the fragments and also for providing an independent and direct physical measurement of the nuclear charge of the fissioning nucleus.

## B. X-Ray Yield and Emission Times

The total number  $N_x$  of the x rays associated with each of the observed peaks was obtained by subtracting the background counts and correcting for the detection efficiency  $\eta_T(E)$ . The background counts outside the x-ray peak were found to decrease nearly linearly with the channel number and, therefore, the background counts  $N_{c_i}$  in any channel  $c_i$  were estimated assuming the relation,  $N_{c_i} = N_0 - mc_i$ . The constants  $N_0$  and  $m$  were determined from the observed counts in the higher channels above the x-ray peak. In addition to this background, a fraction of the x rays undergoing Compton scattering in the crystal, produced a small tail at the low-energy end of the x-ray peaks. The actual number of counts at the low-energy ends of the peaks were, therefore, obtained by comparison with the computed shapes of these distributions.

The average solid angles of detection and half-lives for x-ray emission were obtained from the measured numbers of x rays in the following manner. The numbers  $N_1$  and  $N_2$  of the x rays reaching the x-ray detector were obtained for the cases when the fragments of mass  $M_f$  were moving toward and away from the detector, respectively. The x-ray intensity ratios  $N_1/N_2$  were, then, calculated using the experimental geometry for a range of different fragment velocities and values of  $\lambda$ . From these calculations the values of  $\lambda$  (and de-

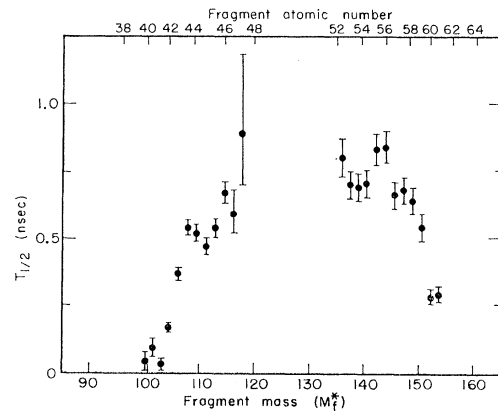


FIG. 6. The average half-life for the  $K$  x-ray emission versus the final masses and atomic numbers of the fragments, as estimated from the analysis of the intensity ratios of the x rays, on the assumption that the x-ray emission is of exponential nature with a single decay constant.

tection geometry) were obtained which gave the observed<sup>15</sup> intensity ratios for the corresponding fragment velocities. Figure 6 shows the average half-lives for the emission of  $K$  x rays from different fragment masses as obtained from the above analysis. On the basis of these estimated half lives, it follows that about 20% of the x rays are emitted within 0.1 nsec, another 57% are emitted within 0.1 to 1.0 nsec, and the remaining 23% are emitted between 1.0 and 50 nsec. These values should be taken only as a rough estimate because we have assumed an exponential relationship with a single decay constant  $\lambda$ . These estimated times of x-ray emission are in fair agreement with a direct measurement of the time of x-ray emission from all the fragments as reported by Glendenin and Griffin,<sup>5</sup> and by Thomas *et al.*<sup>16</sup> In addition, the present measurements give information on the variation of the average half-life of x-ray emission with the fragment mass.

The number of x rays emitted per fragment was obtained from the measured x-ray yield after taking into account the detection efficiency, calculated geometry and the fragment yield. Figure 7 shows the number of x rays per fragment as a function of the fragment mass (corrected for mass dispersion). The total yield of the  $K$  x rays emitted in the time interval 0–50 nsec was found to be  $(0.56 \pm 0.04)$  per fission, the contribution from the light and the heavy group being  $(0.24 \pm 0.02)$  and  $(0.32 \pm 0.02)$ , respectively. The total  $K$  x-ray yield obtained from the present measurements is in good agreement with the value  $(0.57 \pm 0.06)$  measured in the interval 0–150 nsec and corrected for further decay) reported by Glendenin and Griffin,<sup>5</sup> but the relative contribution to the x-ray yield from the light and heavy fragment of  $(0.16 \pm 0.02)$  and  $(0.4 \pm 0.02)$ , respectively reported by them, differ slightly from the present results.

#### IV. DISCUSSION

The division of nuclear charge in fission has in the past been discussed in terms of various relationships which are, mainly, empirical. A comparison of the results of our experiments with those calculated from these various relationships is shown in Fig. 5. Though none of the empirical relations fit the data well, the curve calculated on the equal-charge-displacement

<sup>15</sup> The observed intensity ratio,  $N_1/N_2$ , was corrected for a small difference of the order of a few percent arising in  $N_1$  and  $N_2$  due to the motion of the fragments.

$$\left(\frac{N_1}{N_2}\right)_{\text{corrected}} \approx \left(\frac{N_1}{N_2}\right)_{\text{obs}} \left\{ \frac{(1-\beta_e)^2}{(1+\beta_e)^2} \right\},$$

where  $2\beta_e$  is the observed fractional Doppler shift in the energies of the x rays emitted in and opposite to the direction of motion of the fragments.

<sup>16</sup> T. D. Thomas, R. A. Atneosen, W. M. Gibson, and M. L. Perlman, Proceedings of the International Symposium on the Physics and Chemistry of Fission, Salzburg, Austria, 1965 (unpublished).

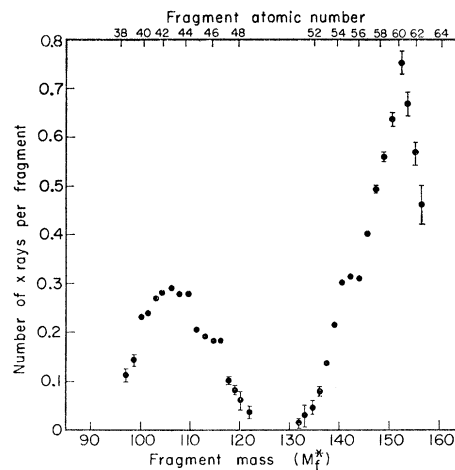


Fig. 7. The observed yield of the prompt  $K$  x rays per fragment emitted in times from 0–50 nsec, versus the final masses ( $M_f^*$ ) and atomic numbers of the fragments (corrected for mass dispersion).

(ECD) hypothesis<sup>17,18</sup> (which assumes that the fragments are equally displaced from the line of  $\beta$  stability) appears to be closest to the experimental results. However, since the ECD hypothesis is not based on a theoretical treatment of charge division, the agreement may be fortuitous and should not be regarded as especially significant.

In order to compare our results with radiochemical data on  $^{252}\text{Cf}$  and with similar data for the thermal fission of  $^{235}\text{U}$  given by Wahl *et al.*,<sup>1</sup> we chose to plot the values of  $\{Z_p - (Z/A)A_i\}$  as a function of mass ratio, where  $Z$  and  $A$  are the charge and mass of the fissioning nucleus and  $Z_p$  is the measured most probable charge of the fragment of initial mass  $A_i$ . This plot is shown in Fig. 8. The figure shows certain facts which may be significant, namely: (1) Although light fragments always have a higher charge density than the heavy fragments, the same trend is not always true within each group itself. In the range of mass ratios from 1.45 to 1.75, the charge density of the light fragments increases with the increase in the mass; (2) over the same range of mass ratio (1.45–1.75), we find there is surprisingly good agreement in the  $^{252}\text{Cf}$  and  $^{235}\text{U}$  results plotted in this way.

The reasons for these phenomena are not understood. One may hope that an adequate understanding of the processes involved in the determination of the nuclear charge distribution will come about through the development of a comprehensive theory of mass and charge division in fission, which at this time does not seem to exist.

<sup>17</sup> L. E. Glendenin, C. D. Coryell, and R. R. Edwards, in *Radiochemical Studies: the Fission Products*, edited by C. D. Coryell and N. Sugarman (McGraw-Hill Book Company, Inc., New York, 1951), p. 489.

<sup>18</sup> A. C. Pappas, *Proceedings of the First United Nations Conference on the Peaceful Uses of Atomic Energy, Geneva, 1955* (United Nations, Geneva, 1955), Vol. 7, p. 19.

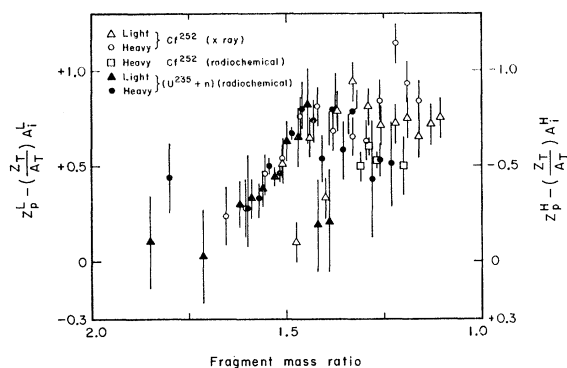


FIG. 8. The deviation of the measured charges from the unchanged charge density curve versus the fragment mass ratio plotted on a complementary scale for the light and heavy fragments. The four square points correspond to the radiochemical measurements of the fragment charges for the spontaneous fission of  $^{252}\text{Cf}$ . The results of the radiochemical measurements of the fragment charges in the thermal neutron fission of  $^{235}\text{U}$  are also shown in the figure. All the radiochemical data is taken from the work of Wahl *et al.* (Ref. 1).

In the following passages, the observations connected with the emission of the  $K$  x rays are discussed. In considering the average yield and time of emission of the  $K$  x rays, one has to consider the mechanism that produces the  $K$  vacancies. The three possibilities are (1) the disruption of the electron cloud during the fission act itself, (2) internal-conversion process during the de-excitation of the fragments and (3) the stopping of the fragments in the fission detectors. The time of emission of the scission x rays is expected<sup>10</sup> to be less than about  $10^{-14}$  sec, and these x rays would, therefore, appear to be coming directly from the source foil. The  $K$  x rays associated with the stopping of fragments would have times of emission of about 2 nsec which is the average time of flight of the fragments to the fission detectors. It has been mentioned earlier that the results shown in Figs. 4 and 6 demonstrate that these x rays are emitted all along the fragment flight path, which is what we expect for the case of internal conversion. Furthermore, the average time of emission of the x rays ( $10^{-10}$ – $10^{-9}$  sec) is found to be comparable to that observed<sup>19,20</sup> for the emission of low-energy gamma rays. One might also expect that variation of the x-ray intensity with fragment mass to be either constant or at least smooth, if the x rays were emitted in the processes (1) and (3). The observed x-ray yield curve (Fig. 7) certainly demonstrates neither of these properties and is what one might expect for the internal-conversion process. These arguments are given further weight by the calculation of Bohr<sup>21</sup> according to which the  $K$  vacancies are not expected either in the fission

act or during the stopping of the fragments in the silicon detector, since the fragment velocities are much less than the velocities of the  $K$  electrons. On the basis of the above experimental facts and the theoretical considerations, it is reasonable to assume that the internal conversion during the gamma de-excitation of the fragments is the main process giving rise to the emission of the  $K$  x rays.

In considering the average time of emission and the yield of these x rays as measured by our method, it is necessary to keep in mind that each mass interval includes not only a range of mass numbers, but also different mass types as well (even-even, even-odd, odd-even, odd-odd). On the basis that these x rays are the result of the internal-conversion process, the x-ray yield curve is expected to be a consequence of a combination of complex effects due to the variation of the number, energy, and multipolarity of the gamma-ray transitions and the fluorescent yield with the fragment mass and charge. The number of  $K$  vacancies per fragment was calculated from our data using the fluorescent yields given by Wapstra *et al.*<sup>10</sup> and are shown by the dotted curve in Fig. 9. The average number of  $K$  vacancies per fission is found to be  $0.32 \pm 0.02$  for the light group and  $0.36 \pm 0.03$  for the heavy group.

An interpretation of the observed electron yield curve (and x-ray yield curve) would require knowledge of the gamma transitions in the fragment nuclei, about which very little is known at present as these nuclei lie in the normally inaccessible neutron-rich region. There are, however, certain general conclusions which may be reached concerning the shape of the yield curve. It is seen that the x-ray yield is minimum in the region of masses approaching symmetry. This region is near the doubly-closed shell with 50 protons and 82 neutrons, and the stable shape of these nuclei should be nearly spherical. The higher transition energies and the low number of transitions in this region, therefore, is expected to give low conversion yields. In moving away from this closed-shell region, in both directions, one may expect the nuclear deformation to increase and give rise to transitions of lower energies, with a consequent increase in the probability of internal conversion as observed. The expected nuclear deformations of these nuclei as given by the mass formula of Myers and Swiatecki<sup>22</sup> confirm this trend and are shown as the solid curve in Fig. 9. In the light fragment group a maximum in the number of  $K$  vacancies is reached near mass 106, which nearly corresponds to the region of maximum fission yield. This can be taken as an evidence that these neutron-rich light fragments, in fact, make up a new region of deformed nuclei. The observed decrease in the number of  $K$  vacancies for the lightest fragments is not, at this stage, understood on the basis of this simple picture. In the heavy group

<sup>19</sup> S. Desi, A. Lajtai, and L. Nagy, *Acta Phys. Hung.* **15**, 185 (1962).

<sup>20</sup> Sven A. E. Johansson, *Nucl. Phys.* **60**, 378 (1965).

<sup>21</sup> N. Bohr, *Phys. Rev.* **59**, 270 (1941).

<sup>22</sup> W. Myers and W. J. Swiatecki (private communication).

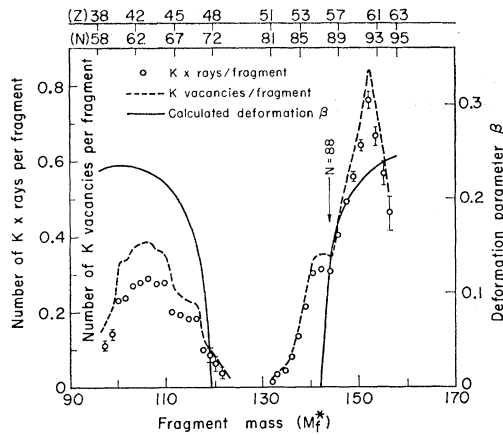


FIG. 9. Calculated number of  $K$  vacancies per fragment (as obtained using the x ray data and the fluorescent yield) versus the final fragment mass,  $M_f^*$ , and the most probable neutron and proton numbers. The expected nuclear deformation parameter,  $\beta$ , of these fragment nuclei as calculated by the mass formula of Myers and Swiatecki (Ref. 22) is also plotted in the figure.

the peak in the yield curve near mass 152 is about 7 mass units above the region of the most probable heavy fragments. The abrupt rise in the  $K$ -electron yield for fragment masses greater than 144 is very likely connected with the onset of large nuclear deformation at neutron number 88. In particular, if one considers only the transitions in even-even nuclei, the lowering in the energy of the first and second excited states ( $2^+, 4^+$ ) at about 88 to 90 neutrons is expected to contribute a considerable increase in the conversion coefficients. The decrease in the number of  $K$  vacancies for fragment masses greater than 152 may be the result

of an increase in the effective transition energies or decrease in the number of effective transitions both being affected by the relative contributions of nuclei of different kinds, but the underlying reasons are not clear at present.

In conclusion it may be stated that a detailed understanding of these complicated effects would require further investigation and should not be expected on the basis of the results of this preliminary experiment which had, at least in the beginning, a much more limited objective. However, it may be stated that the study of these x rays seems to offer another means for obtaining information about the gamma-ray transitions in these neutron-rich fragment nuclei. It appears that simultaneous measurements of  $K$  x rays, conversion electrons and gamma rays should be able to provide more comprehensive information about the properties of these nuclei.

#### ACKNOWLEDGMENTS

We are thankful to Richard C. Jared for his valuable help in carrying out the experiments, and to Michiyuki Nakamura and his group for their help in the maintenance of the multiparameter analyzer and the associated systems. Our thanks are due J. O. Rasmussen and W. J. Swiatecki for many helpful discussions. We gratefully acknowledge the valuable assistance of Joan Phillips during the preparation of the manuscript. One of us (S. S. Kapoor) wishes to thank the Agency for International Development, Washington, Lawrence Radiation Laboratory, Berkeley, and the U. S. Atomic Energy Commission for providing the opportunity to work at the Lawrence Radiation Laboratory, Berkeley.



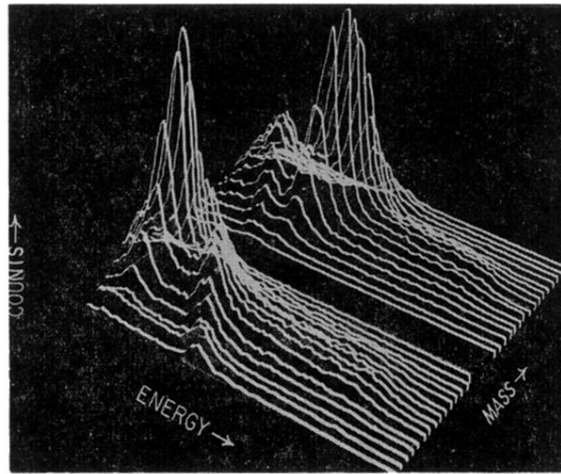


FIG. 3. A three-dimensional model of the observed energy spectra of the prompt  $K$  x rays for 36 intervals of the fragment masses moving toward the x ray detector.